Fermi National Accelerator Laboratory

FERMILAB-Pub-98/037-A

# Implications for the Hubble Constant from the First Seven Supernovae of $z \geq 0.35$

A.G. Kim et al.
The Supernova Cosmology Project

*Fermi National Accelerator Laboratory*
*P.O. Box 500, Batavia, Illinois 60510*

January 1998

Submitted to *Astrophysical Journal, Letters*

Operated by Universities Research Association Inc. under Contract No. DE-AC02-76CH03000 with the United States Department of Energy

## Disclaimer



## Distribution

# Implications For The Hubble Constant from the First Seven Supernovae of $z \geq 0.35$

A. G. Kim,[1,2] S. Gabi,[1,3] G. Goldhaber,[1,2] D. E. Groom,[1] I. M. Hook,[2,10] M. Y. Kim,[1] J. C. Lee,[1] C. R. Pennypacker,[1,3] S. Perlmutter,[1,2] I. A. Small,[1,2] A. Goobar,[2,4] R. Pain,[5] R. S. Ellis,[6] R. G. McMahon,[6] B. J. Boyle,[7,8] P. S. Bunclark,[7] D. Carter,[7] M. J. Irwin,[7] K. Glazebrook,[8] H. J. M. Newberg,[9] A. V. Filippenko,[10] T. Matheson,[10] M. Dopita,[11] and W. J. Couch[12]

(The Supernova Cosmology Project)

Received _____; accepted _____

[1]E. O. Lawrence Berkeley National Laboratory, Berkeley, California 94720; agkim@LBL.gov

[2]Center for Particle Astrophysics, U.C. Berkeley, California 94720

[3]Space Sciences Laboratory, U.C. Berkeley, California 94720

[4]University of Stockholm

[5]CNRS-IN2P3, University of Paris

[6]Institute of Astronomy, Cambridge, United Kingdom

[7]Royal Greenwich Observatory, Cambridge, United Kingdom

[8]Anglo-Australian Observatory, Sydney, Australia

[9]Fermilab, Batavia, Illinois 60510

[10]University of California, Berkeley, California 94720

[11]Mt. Stromlo and Siding Springs Observatory, Australia

[12]University of New South Wales, Sydney, Australia

## ABSTRACT

The Supernova Cosmology Project has discovered over twenty-eight supernovae (SNe) at $0.35 < z < 0.65$ in an ongoing project that uses Type Ia SNe as high-redshift distance indicators. We here present measurements of the ratio between the locally observed and global Hubble constants, $H_0^L/H_0^G$, based on the first 7 SNe of this high-redshift data set compared with 18 SNe at $z \leq 0.1$ from the Calan/Tololo data set. If $\Omega_M \leq 2$, then light-curve-width corrected SN magnitudes yield $H_0^L/H_0^G < 1.20$ (95% confidence level) in a $\Lambda = 0$ universe and $H_0^L/H_0^G < 1.27$ in a flat universe. The analysis using the Type Ia as a standard candle without a light-curve-shape correction yields similar results. Using the Cepheid-distance-calibrated absolute magnitudes for SNe Ia of Sandage et al. (1996), we can also measure the global Hubble constant, $H_0^G$. Independent of $\Omega_M$, we find that $H_0^G < 71$ km s$^{-1}$ Mpc$^{-1}$ in a $\Lambda = 0$ universe and $H_0^G < 83$ km s$^{-1}$ Mpc$^{-1}$ in a flat universe correcting the distant and local SN apparent magnitudes for light curve width. Lower results for $H_0^G$ are obtained if the magnitudes are not width corrected.

## 1. Introduction

Some of the recent Cepheid measurements in galaxy clusters suggest a high value of the Hubble constant, $69 \leq H_0 \leq 87$ km s$^{-1}$Mpc$^{-1}$ (e.g. Pierce et al. 1994; Freedman et al. 1994; Tanvir et al. 1995). However, if the cosmological constant is zero such a large Hubble constant will predict an age of the universe that is lower than the calculated ages of globular cluster stars (Bolte & Hogan 1995). To account for this discrepancy, it has been proposed that the locally ($z \leq 0.05$) observed Hubble constant, $H_0^L$, is actually higher than the global ($z > 0.3$) Hubble constant, $H_0^G$ (Bartlett et al. 1995). Alternatively, it may be that these Hubble constant measurements lie on the tail of their statistical/systematic error distributions. We use our first sample of seven $z > 0.35$ SNe to address both these possibilities, first by directly comparing our SN sample with one lying within the local Hubble flow to determine the ratio of $H_0^L$ to $H_0^G$, and then by using our sample (the first SNe observed in this redshift regime) together with Type Ia absolute magnitude calibrations to determine $H_0^G$.

The possibility that $H_0^L/H_0^G \neq 1$ has arisen in the context of the observation of peculiar velocity fields. The results of de Vaucouleurs (1958), Dressler et al. (1987), and Lynden-Bell et al. (1988) suggest that local measurements of the Hubble constant may differ from the mean global value. Simulations of Turner, Cen, & Ostriker (1992) have shown that measured Hubble constants depend on the observer location and the depth of observations. Previous work by Lauer & Postman (1992) has constrained deviations from uniform Hubble flow to be $\Delta H_0/H_0 < 0.07$ at redshifts $0.01 \leq z \leq 0.05$ using Brightest Cluster Galaxies as a distance indicator. However, the same sample of galaxies shows evidence for a peculiar motion of 689 km s$^{-1}$ with respect to the cosmic background radiation (Lauer & Postman 1994), although Riess, Press, & Kirshner (1995a) argue that SNe at similar redshifts do not support this conclusion. We thus must still examine the possibility of a large scale

($z \geq 0.05$) peculiar velocity flow affecting all the local $H_0$ measurements.

The Supernova Cosmology Project has discovered over twenty-eight SNe in a redshift range $0.35 < z < 0.65$ in a systematic search (Perlmutter et al. 1994; 1995). This new sample of SNe is a potentially valuable tool for cosmology: the peak magnitudes of these high-redshift standard candles, when compared with the peak magnitudes of local SNe, can yield measurements of the cosmological parameters $\Omega_M$ and $\Lambda$ (Goobar & Perlmutter 1995, Perlmutter et al. 1996b). This calculation implicitly assumes that the local SN calibrators lie within the global cosmological flow; i.e. that we do not live in a local bubble where peculiar velocities appreciably bias the observed value of the Hubble constant. In this paper (Section 3) we take an alternative approach, leaving $\Omega_M$ and $\Lambda$ as free parameters and using our high redshift SNe to measure the ratio between the locally observed Hubble constant and the global Hubble constant, $H_0^L/H_0^G$.

We also use our SNe to obtain a measurement of the Hubble constant (Section 4). This can be compared to the other SN-based measurements which range from 57 km s$^{-1}$Mpc$^{-1}$ (Sandage et al. 1996) to $\sim$ 66 km s$^{-1}$Mpc$^{-1}$ (Hamuy et al. 1995, Riess, Press, & Kirshner 1996), and to the Cepheid methods mentioned above that must bootstrap distances in a sequence from a single galaxy, to the core of its cluster, and then to the Coma cluster.

## 2. Our distant sample

We have developed and implemented a systematic search for SNe at redshifts $> 0.3$. The first seven SNe from this search were discovered between 1992 and 1994, on the rising side of their light curves. For these SNe we obtained follow-up photometry and spectroscopy of the SN and its host galaxy. A detailed description of our search methodology, the telescopes used, the data compiled for each event, and light curve analysis, are given in

Perlmutter et al. (1996a; 1996b).

Table 1 summarizes the properties of our SNe that are relevant to this paper: the redshift as measured from the host galaxy spectrum, the best fit K-corrected $B$ peak magnitude after our galaxy extinction correction, $m_B = m_R - K_{BR} - A_R$, the $\Delta m_{15}$, and $m_B$ after correction to the Leibundgut template, $m_B^{\{1.1\}}$, using the relation of Hamuy et al. (1996), discussed in Section 3. For this paper, we take these seven SNe to be Type Ia with no evolutionary effects. For a detailed discussion on the evidence for the Type Ia classification, see Perlmutter et al. (1996b).

## 3. The determination of $H_0^L/H_0^G$

In order to use Type Ia SNe as a standard candle, we first must calibrate their luminosities. If the absolute distance to a SN is known, e.g. from Cepheids in the same galaxy, then we can obtain the absolute magnitude $M$ from the apparent magnitude $m$. More commonly, we can only measure the redshift and an apparent magnitude. From these quantities we can obtain the intercept $\mathcal{M}$ of the magnitude axis of the Hubble relationship, $m = 5 \log cz + \mathcal{M}$. (Following the notation of Perlmutter et al. 1996b, the script variable indicates a quantity that can be measured without knowing $H_0$ or the absolute distance.) These two independent observables are related at low redshifts by the following relation:

$$\mathcal{M} = M - 5 \log H_0 + 25, \tag{1}$$

where $H_0$ is in units of km s$^{-1}$Mpc$^{-1}$. We call $\mathcal{M}$ the "Hubble intercept" magnitude or the "magnitude zero point" and we use it instead of $M$ when studying relative values of the Hubble constant.

Progress has been made in determining both $M$ and $\mathcal{M}$ using nearby supernovae. The Calan/Tololo Supernova Search has discovered and measured a large sample of Type

Ia's within the local Hubble flow, from which a Hubble diagram with narrow magnitude dispersion can be produced and the Hubble intercept $\mathcal{M}$ fitted. The sample includes 18 SNe discovered within 5 days of maximum or sooner with redshifts ranging from $3.6 < \log(cz) < 4.5$. (Of these, half are objects with $cz > 15000$ km s$^{-1}$, beyond the distance of the Lauer & Postman (1994) galaxy cluster sample. However, these SNe have magnitudes consistent with the ones at lower redshift.) Using these 18 supernovae, Hamuy et al. (1996) find

$$\mathcal{M}_B = -3.17 \pm 0.03 \tag{2}$$

with rms dispersion $\sigma = 0.26$.

Recent advances have lead to a more detailed understanding of Type Ia SNe: there is now compelling evidence that SNe Ia represent a family rather than a unique set of objects. A correlation between peak magnitude and light-curve shape has been found; Phillips (1993) and Hamuy et al. (1995) parameterize the light curve with the $B$-band magnitude difference between peak and 15 days after peak, $\Delta m_{15}$; Riess, Press, & Kirshner (1995b; 1996) characterize the light-curve shape by the amount, $\Delta$, of a correction template needed to be added to a Leibundgut et al. (1991) template to get a best $\chi^2$ fit. These parameterizations within the Type Ia class, as well as those involving spectral features (Fisher et al. 1995; Nugent et al. 1995) may make it possible to use the Type Ia as a "calibrated" candle with $B$ magnitude dispersions of $< 0.2$ mag.

The Hamuy et al. (1996) sample gives a linear relation between $\Delta m_{15}$ and the magnitude of the supernova, which can be expressed in terms of the Hubble intercept:

$$\mathcal{M}_{B,corr} = (0.86 \pm 0.21)(\Delta m_{15} - 1.1) - (3.32 \pm 0.05). \tag{3}$$

This relation is used to "correct" observed SN magnitudes to a $\Delta m_{15} = 1.1$ standard template magnitude, $\mathcal{M}_B^{\{1.1\}}$. Applying this correction reduces the rms dispersion to $\sigma = 0.17$ for the observed range of $\Delta m_{15}$, between 0.8 and 1.75.

Not all SN samples show a strong correlation between light-curve shape and peak magnitude. Sandage et al. (1996) cite the apparent lack of such a relation in the Cepheid calibrated SNe to argue for the use of non-corrected "Branch-normal" SNe Ia, i.e. SNe with high quality data that pass a simple $B-V$ color selection or have no spectroscopic peculiarities. This subset of SNe also have a low dispersion in $B$ magnitude of $\sim 0.3$ mag, as shown in Vaughan et al. (1995). For this paper we therefore calculate $H_0^L/H_0^G$ using both light-curve shape corrected and non-corrected magnitudes.

We relate the locally derived values of the Hubble intercept and the high-redshift observed magnitudes using the standard Friedmann-Lemaître cosmology in order to measure $H_0^L/H_0^G$. The expected peak magnitude of a Type Ia SN at redshift $z$ is a function of the mass density of the universe $\Omega_M$ and the normalized cosmological constant $\Omega_\Lambda \equiv \Lambda/(3H_0^2)$ :

$$m_R(z) = M_B + 5\log(\mathcal{D}_L(z;\Omega_M,\Omega_\Lambda)) + K_{BR} + 25 - 5\log H_0^G \quad (4)$$

$$= \mathcal{M}_B + 5\log(\mathcal{D}_L(z;\Omega_M,\Omega_\Lambda)) + K_{BR} + 5\log(H_0^L/H_0^G), \quad (5)$$

where $K_{BR}$ is the K correction relating $B$ magnitudes of nearby SNe with $R$ magnitudes of distant objects (Kim, Goobar, & Perlmutter 1996) and $\mathcal{M}_B$ is measured in the local Hubble flow. We here use $\mathcal{D}_L$, the "Hubble-constant-free" part of the luminosity distance, $d_L$:

$$\mathcal{D}_L(z;\Omega_M,\Omega_\Lambda) \equiv d_L H_0 = \frac{c(1+z)}{\sqrt{|\kappa|}} \quad \mathcal{S}\left(\sqrt{|\kappa|}\int_0^z \left[(1+z')^2(1+\Omega_M z') - z'(2+z')\Omega_\Lambda\right]^{-\frac{1}{2}} dz'\right) \quad (6)$$

where for $\Omega_M + \Omega_\Lambda > 1$, $\mathcal{S}(x)$ is defined as $\sin(x)$ and $\kappa = 1 - \Omega_M - \Omega_\Lambda$; for $\Omega_M + \Omega_\Lambda < 1$, $\mathcal{S}(x) = \sinh(x)$ and $\kappa$ as above; and for $\Omega_M + \Omega_\Lambda = 1$, $\mathcal{S}(x) = x$ and $\kappa = 1$, where $c$ is the speed of light in units of km s$^{-1}$. We express $\mathcal{M}_\mathrm{B}$ with Equation 2 for non-corrected magnitudes, and Equation 3 for light-curve-shape corrected magnitudes. For the high-redshift corrected SN magnitudes, $m_R$, we use only the five SNe whose light-curve shapes lie within the range ($0.8 < \Delta m_{15} < 1.75$) of the local SNe from which the correlation was obtained; SN1994G, SN1994H, SN1994al, SN1994am, and SN1994an. The full sample of

high-redshift SNe is used when no correction is applied.

Figure 1 shows the best fit values of $H_0^L/H_0^G$ and the associated confidence interval curves for a range of $\Omega_M$ in a $\Lambda = 0$ universe, based on the light-curve-width corrected SN magnitudes. Figure 2 is the same plot as Figure 1 but for the case of a flat universe ($\Omega_M + \Omega_\Lambda = 1$). Note that the best fit curve is more steeply sloped than for the $\Lambda = 0$ case, increasing the variation in $H_0^L/H_0^G$ in this $\Omega_M$ range. (The same plots for the seven non-corrected magnitudes are almost identical on this scale.)

Table 2 has the single-tailed 95% confidence limits for $H_0^L/H_0^G$ in $\Lambda = 0$ and flat universes using corrected and non-corrected SN magnitudes. The lower bounds are calculated at $\Omega_M = 0$ where $H_0^L/H_0^G$ is a minimum. $H_0^L/H_0^G$ increases monotonically with respect to $\Omega_M$, so to obtain an upper limit we choose an upper bound of $\Omega_M \leq 2$. Note that the tabulated numbers are one-tailed 95% C.L. limits, unlike the two-tailed confidence intervals given in Figures 1 and 2.

As a cross check, we calculate our results for "Branch-normal" SNe with uncorrected magnitudes. Only SN1994G and SN1994an are confirmed "Branch-normal" based on their color or spectrum. The results obtained when using only these two are statistically consistent with that of the full sample. In a $\Lambda = 0$ universe, we here obtain the limits $H_0^L/H_0^G > 0.79$ and $H_0^L/H_0^G < 1.27$, for a flat universe we obtain $H_0^L/H_0^G > 0.68$ and $H_0^L/H_0^G < 1.35$.

In the most general case with $\Omega_M$ and $\Omega_\Lambda$ independent and unconstrained, we use Equation 5 to calculate $H_0^L/H_0^G$ for different values of $\Omega_M$ and $\Omega_\Lambda$. Figure 3 shows curves of constant $H_0^L/H_0^G$ and associated uncertainties on the $\Omega_M - \Omega_\Lambda$ plane as calculated from the five corrected SN magnitudes. Given in parentheses on the same plot are the $H_0^L/H_0^G$ values for the same contours based on calculations from all seven non-corrected SN magnitudes. (The corrected and non-corrected contours do not have the exact same shape

in the $\Omega_M - \Omega_\Lambda$ plane due to their redshift dependence. However, their actual deviations are small within the scale of our plot and given our error bars. We thus present the results from both scenarios in a single plot.) Within the region plotted, $H_0^L/H_0^G = 70/50 = 1.4$ is excluded to $\gg 99\%$ confidence. This limit can still be lower if independent lower limits of the age of the universe and $\Omega_\Lambda$ are included.

In Perlmutter et al. (1996b), we discuss the potential errors due to Malmquist bias and host galaxy extinction. The bounds on those errors are small enough not to affect our results.

## 4. The Hubble Constant

The measurement of the Hubble constant $H_0^G$, as opposed to the ratio of Hubble constants $H_0^L/H_0^G$, requires the absolute magnitude $M$. The high-resolution of the Hubble Space Telescope has made possible the discovery and measurement of Cepheid light curves in galaxies that have hosted well-observed Type Ia supernovae (Sandage et al. 1996; Saha et al. 1994; Saha et al. 1995). To date, six galaxy distances have been calculated to determine the peak absolute magnitudes of seven supernovae. The weighted mean of these SN magnitudes is given in Sandage et al. (1996) as

$$M_B = -19.47 \pm 0.07 \tag{7}$$

with a dispersion $\sigma = 0.16$.

Six of the seven SNe have a $\Delta m_{15}$ measurement (Sandage et al. 1996), from which we calculate the weighted mean of the peak absolute magnitude of SNe corrected to $\Delta m_{15} = 1.1$. Using the $\Delta m_{15}$- magnitude relation of Equation 3 we find

$$M_B^{\{1.1\}} = -19.45 \pm 0.07 \tag{8}$$

with $\sigma = 0.14$.

There is some debate on whether these SNe have been properly extinction-corrected and weighted. For example, Riess, Press, & Kirshner (1996) using the correction template method mentioned above, conclude that SN1972E is significantly extincted by its host galaxy. It has also been noted that the SNe measured with photographic plates give magnitudes that are systematically brighter than ones measured photoelectrically. Therefore, although we use all seven (six for the $\Delta m_{15}$ corrected) SNe for our main results, we also include for comparison the Riess, Press, & Kirshner (1996) analysis of the three SNe with photoelectric data that yields:

$$M_{B,\Delta=0} = -19.36 \pm 0.1 \tag{9}$$

for a $\Delta = 0$ Leibundgut template supernova.

Inserting the absolute magnitudes of Equations 7 and 8 into Equation 4, we obtain useful upper bounds of the Hubble constant, which are listed in Table 2. The bounds are calculated at $\Omega_M = 0$ for $\Lambda = 0$ universes and flat universes because $H_0^G$ decreases with increasing $\Omega_M$. If we take $\Omega_M \geq 0.2$ we obtain even tighter limits, also given in Table 2. Figure 3 shows $H_0^G$ in the most general case, with $\Omega_M$ and $\Omega_\Lambda$ independent and unconstrained. Note that a value of $H_0$ as high as 80 km s$^{-1}$Mpc$^{-1}$ is only found for large values of $\Omega_\Lambda$ and low $\Omega_M$. As a cross check, we again calculate our results for non-corrected "Branch-normal" supernovae. We then find $H_0^G < 70$ km s$^{-1}$Mpc$^{-1}$ in a $\Lambda = 0$ universe and $H_0^G < 82$ km s$^{-1}$Mpc$^{-1}$ in a flat universe.

## 5. Conclusions

The measurement of cosmological distances using high-redshift SNe with locally-calibrated standard candles sets a limit on the differences between the local and global

Hubble constants. From our analysis, it is clear that this data is inconsistent with scenarios that use a local bubble with high $H_0^L$ that differs greatly from $H_0^G$. We also obtain an upper limit for the Hubble constant that is consistent with many of the other current measurements. However, tighter limits that disagree with some measurements may be obtained with independent constraints on $\Omega_\Lambda$.

The Type Ia absolute magnitude calibrations are still subject to debate and may have systematic errors larger than the statistical ones given above so it is important to ask how robust our results are. An uncertainty in the absolute calibration $\delta m$ in magnitudes propagates into $\delta H_0/H_0 \approx \delta m$. A 0.09 mag difference in the magnitude calibrations, such as the one between the $\Delta m_{15}$-corrected absolute magnitudes for six SNe (Equation 8) and that of Riess, Press, & Kirshner (1996) with their extinction corrections for three of the SNe (Equation 9), will produce a 10% change in either $H_0^G$ or $H_0^L/H_0^G$.

There is little difference between magnitude corrected and non-corrected results for the ratio $H_0^L/H_0^G$, but there is a systematic difference for $H_0^G$ by itself, as seen in Table 2. This is because both the light-curve width distribution and the width-magnitude relation of our high-redshift sample are similar to the distribution and relation of the Hamuy et al. (1996) sample but not to those of the Sandage et al. (1996) sample. Although these differences may be due to selection effects, the small number statistics of the Cepheid-calibrated SN sample can produce fluctuations that account for the differences.

In Perlmutter et al. (1996b) we calculated $\Omega_M$ and $\Omega_\Lambda$ setting $H_0^L$ equal to $H_0^G$ whereas in this paper we have discussed the measurement of $H_0^L/H_0^G$ while leaving $\Omega_M$ and $\Omega_\Lambda$ as free parameters. Ideally one would like to measure both sets of quantities simultaneously. (This problem has been discussed in Wu, Qin, & Fang 1996.) Filling in a Hubble diagram with measurements of spatially well distributed SNe should make it possible to decouple local and global streaming motions by showing redshift dependent deviations from the

standard model, and allow one to measure $\Omega_M$ and $\Omega_\Lambda$ independently of local peculiar flows. Using SNe from redshift regimes with no evidence of flows, we can simultaneously fit $H_0^G$, $\Omega_M$, and $\Omega_\Lambda$ using Equation 4, producing an independent measurement of the Hubble constant. Our current data set, which spans from $0.35 < z < 0.5$, shows no sign of peculiar flows but needs higher statistics and fuller spatial coverage to confirm this result.

This work was supported in part by the National Science Foundation (ADT-88909616) and U. S. Department of Energy (DE-AC03-76SF000098).

## REFERENCES

Bartlett, J. G., Blanchard, A., Silk, J., & Turner, M. S. 1995, Science, 267, 980–983

Bolte, M., & Hogan, C. J. 1995, Nature, 376, 399

de Vaucouleurs, G. 1958, AJ, 63, 253

Dressler, A., Faber, S. M., Burstein, D., Davies, R. L., & Lynden-Bell, D. 1987, ApJ, 313, 37

Fisher, A., Branch, D., Hoflich, P., & Khokhlov, A. 1995, ApJ, 447, L73

Freedman, W. L., Madore, B. F., Mould, J. R., Hill, R., Ferrarese, L., Kennicutt, R. C., Saha, A., Stetson, P. B., Graham, J. A., Ford, H., Hoessel, J. G., Huchra, J., Hughes, S. M., & Illingworth, G. D. 1994, Nature, 371, 757

Goobar, A., & Perlmutter, S. 1995, ApJ, 450, 14

Hamuy, M., Phillips, M. M., Maza, J., Suntzeff, N. B., Schommer, R. A., & Aviles, R. 1995, AJ, 109, 1

Hamuy, M., Phillips, M. M., Schommer, R. A., Suntzeff, N. B., & Maza, J. 1996, AJ in press

Kim, A. G., Goobar, A., & Perlmutter, S. 1996, PASP, 108, 190

Lauer, T., & Postman, M. 1992, ApJ, 400, L47

Lauer, T., & Postman, M. 1994, ApJ, 425, L418

Leibundgut, B., Tammann, G., Cadonau, R., & Cerrito, D. 1991, AAPS, 89, 537

Lynden-Bell, D., Faber, S. M., Burstein, D., Davies, R. L., & Dressler, A. 1988, ApJ, 326, 19L

Nugent, P., Phillips, M., Baron, E., Branch, D., & Hauschildt, P. 1995, ApJ, 455L, 147

Perlmutter, S., Pennypacker, C., Goldhaber, G., Goobar, A., Pain, R., Grossan, B., Kim, A., Kim, M., & Small, I. 1994, International Astronomical Union Circular, nos. 5956 and 5958

Perlmutter, S., Deustua, S., Goldhaber, G., Groom, D., Hook, I., Kim, A., Kim, M., Lee, J., Melbourne, J., Pennypacker, C., Small, I., Goobar, A., Pain, R., Ellis, R., McMahon, R., Boyle, B., Bunclark, P., Carter, D., Irwin, M., Filippenko, A. V., Barth, A., Couch, W., Dopita, M., Mould, J., & York, D. 1995, International Astronomical Union Circular, no. 6270

Perlmutter, S., Deustua, S., Gabi, S., Goldhaber, G., Groom, D., Hook, I., Kim, A., Kim, M., Lee, J., Pain, R. Pennypacker, C., Small, I., Goobar, A., Ellis, R., McMahon, R., Boyle, B., Bunclark, P., Carter, D., Glazebrook, K., Irwin, M., Newberg, H., Filippenko, A. V., Matheson, T., Dopita, M., Mould, J., & Couch, W. 1996a. Analysis paper. In Thermonuclear Supernovae, Dordrecht:Kluwer

Perlmutter, S., Gabi, S., Goldhaber, G., Groom, D., Hook, I., Kim, A., Kim, M., Lee, J., Pennypacker, C., Small, I., Goobar, A., Pain, R., Ellis, R., McMahon, R., Boyle, B., Bunclark, P., Carter, D., Irwin, M., Glazebrook, K., Newberg, H., Filippenko, A. V., Matheson, T., Dopita, M., & Couch, W. 1996b, ApJ Submitted

Phillips, M. M. 1993, ApJ, 413L, 105

Pierce, M. J., Welch, D. L., McClure, R. D., van den Bergh, S., Racine, R., & Stetson, P. B. 1994, Nature, 371, 385

Riess, A. G., Press, W. H., & Kirshner, R. P. 1995a, ApJ, 445, L91

Riess, A. G., Press, W. H., & Kirshner, R. P. 1995b, ApJ, 438, L17

Riess, A. G., Press, W. H., & Kirshner, R. P. 1996, ApJ, in press

Saha, A., Labhardt, L., Schwngeler, H., Macchetto, F. D., Panagia, N., Sandage, A., & Tammann, G. A. 1994, ApJ, 425, 14

Saha, A., Sandage, A., Labhardt, L., Schwngeler, H., Tammann, G. A., Panagia, N., & Macchetto, F. D. 1995, ApJ, 438, 8

Sandage, A., Saha, A., Tammann, G. A., Labhardt, L., Panagia, N., & Macchetto, F. D. 1996, ApJ, 460, L15

Tanvir, N. R., Shanks, T., Ferguson, H. C., & Robinson, D. R. T. 1995, Nature, 377, 27

Turner, E., Cen, R., & Ostriker, J. P. 1992, ApJ, 103, 1427

Vaughan, T., Branch, D., Miller, D., & Perlmutter, S. 1995, ApJ, 439, 558

Wu, X., Qin, B., & Fang, L. 1996, ApJ, in press

Table 1. Supernova Data and Photometry Error Budget

| | SN1992bi | SN1994H | SN1994al | SN1994F | SN1994am | SN1994G | SN1994an |
|---|---|---|---|---|---|---|---|
| $z$ | 0.458 | 0.374 | 0.420 | 0.354 | 0.372 | 0.425 | 0.378 |
| $m_B$ | 22.70 (9) | 21.91 (4) | 22.81 (12) | 22.45 (30) | 22.25 (6) | 22.27 (6) | 22.62 (7) |
| $\Delta m_{15}$ | 0.50 (40) | 0.87(9) | 1.18(20) | 2.00 (61) | 1.44 (12) | 1.05 (3) | 1.64 (29) |
| $m_B^{\{1.1\}}$ | ··· [a] | 22.11 (10) | 22.74 (21) | ··· [a] | 21.96 (13) | 22.32 (7) | 22.16 (28) |

[a]Note SN1992bi and SN1994F have best fit $\Delta m_{15}$ outside the range found for the nearby SNe Ia and therefore, to avoid extrapolation, $m_B^{\{1.1\}}$ corrected magnitudes are not reported or used.

Table 2. The 95% One-Tailed Confidence Levels for $H_0^L/H_0^G$

| | | $H_0^L/H_0^G$ | | $H_0^G$ Upper limit $\frac{\text{km}}{\text{s Mpc}}$ | |
|---|---|---|---|---|---|
| | | Lower Limit | Upper Limit | $\Omega_M \geq 0$ | $\Omega_M \geq 0.2$ |
| $\Lambda = 0$ | Corrected | $> 0.83$ | $< 1.20$ | $< 71$ | $< 70$ |
| | Non-corrected | $> 0.86$ | $< 1.21$ | $< 65$ | $< 63$ |
| $\Omega_M + \Omega_\Lambda = 1$ | Corrected | $> 0.77$ | $< 1.27$ | $< 83$ | $< 78$ |
| | Non-corrected | $> 0.75$ | $< 1.30$ | $< 78$ | $< 70$ |

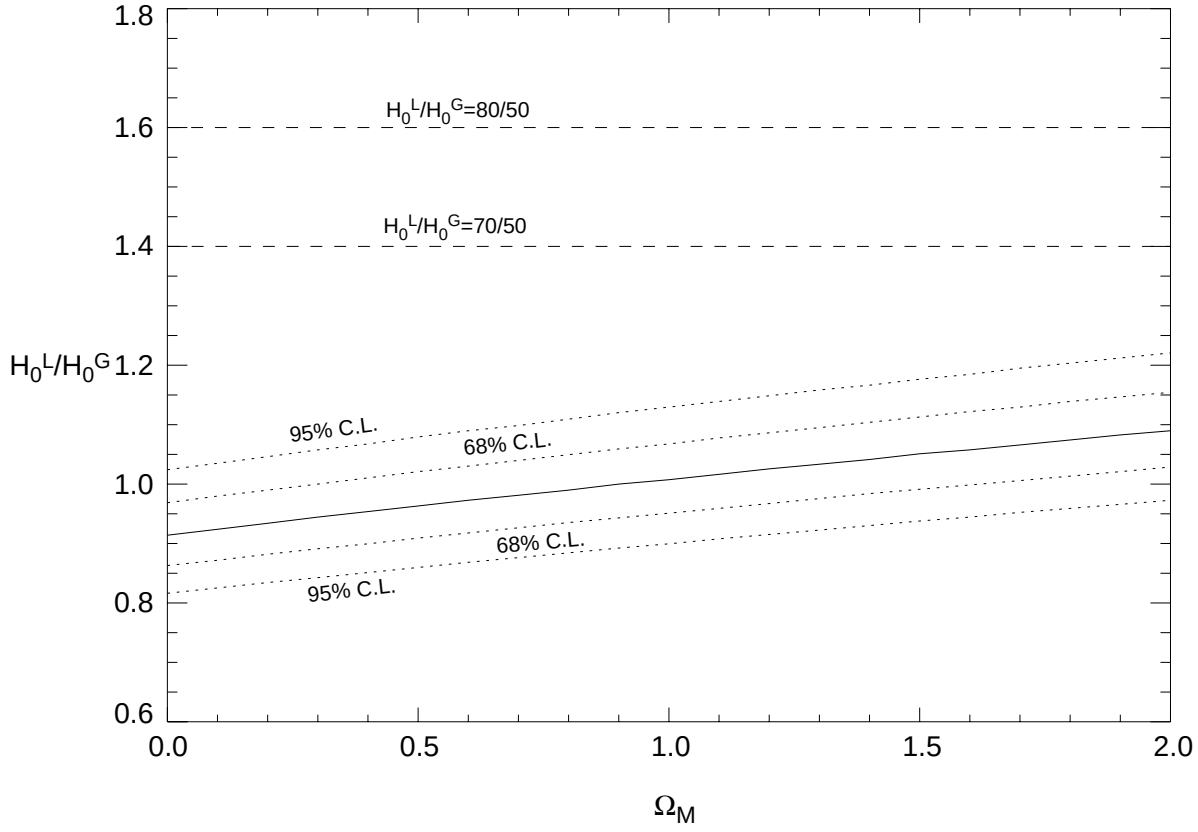


Fig. 1.— The best fit $H_0^L/H_0^G$ with 68% and 95% error range for each value of $\Omega_M$ in a $\Lambda = 0$ universe using the five light-curve corrected SN magnitudes. (These are the results from a single parameter fit, the errors are calculated for each value of $\Omega_M$.)

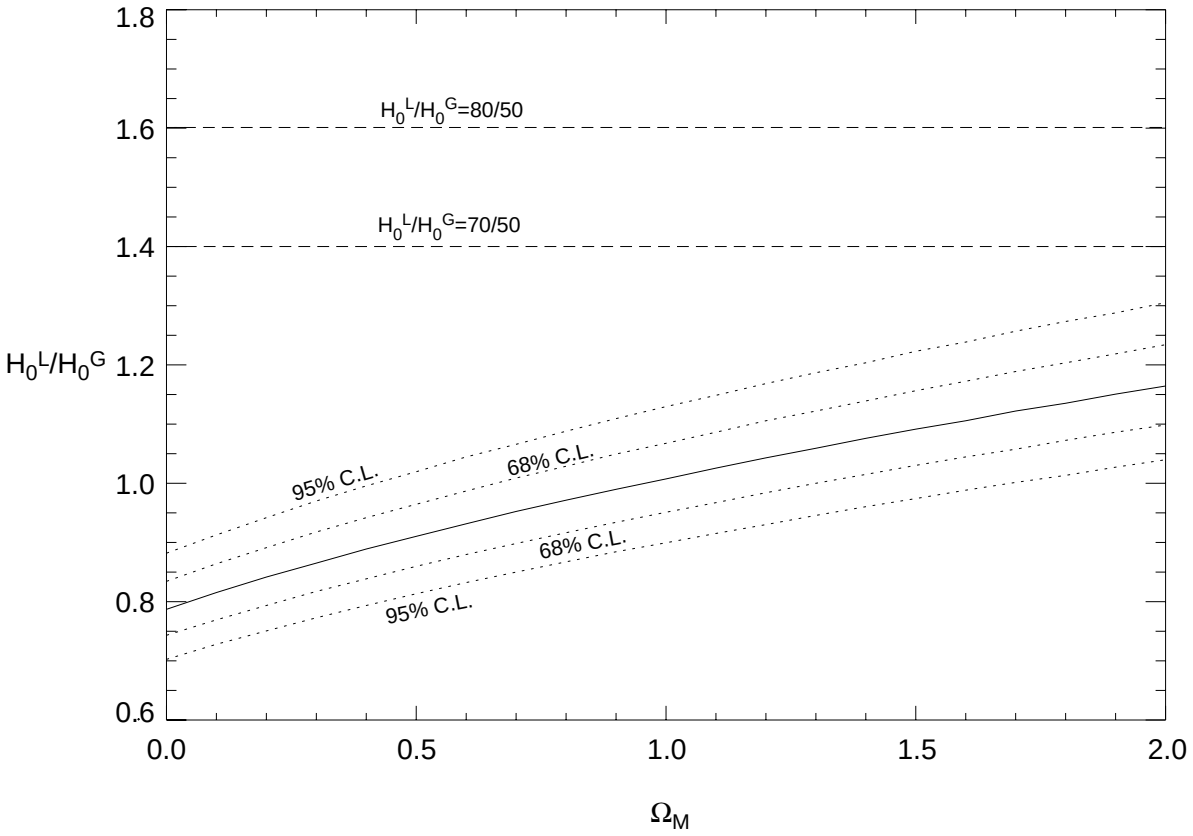


Fig. 2.— The best fit $H_0^L/H_0^G$ with 68% and 95% error range for each value of $\Omega_M$ in a flat universe using the five light-curve corrected SN magnitudes. (These are the results from a single parameter fit, the errors are calculated for each value of $\Omega_M$.)

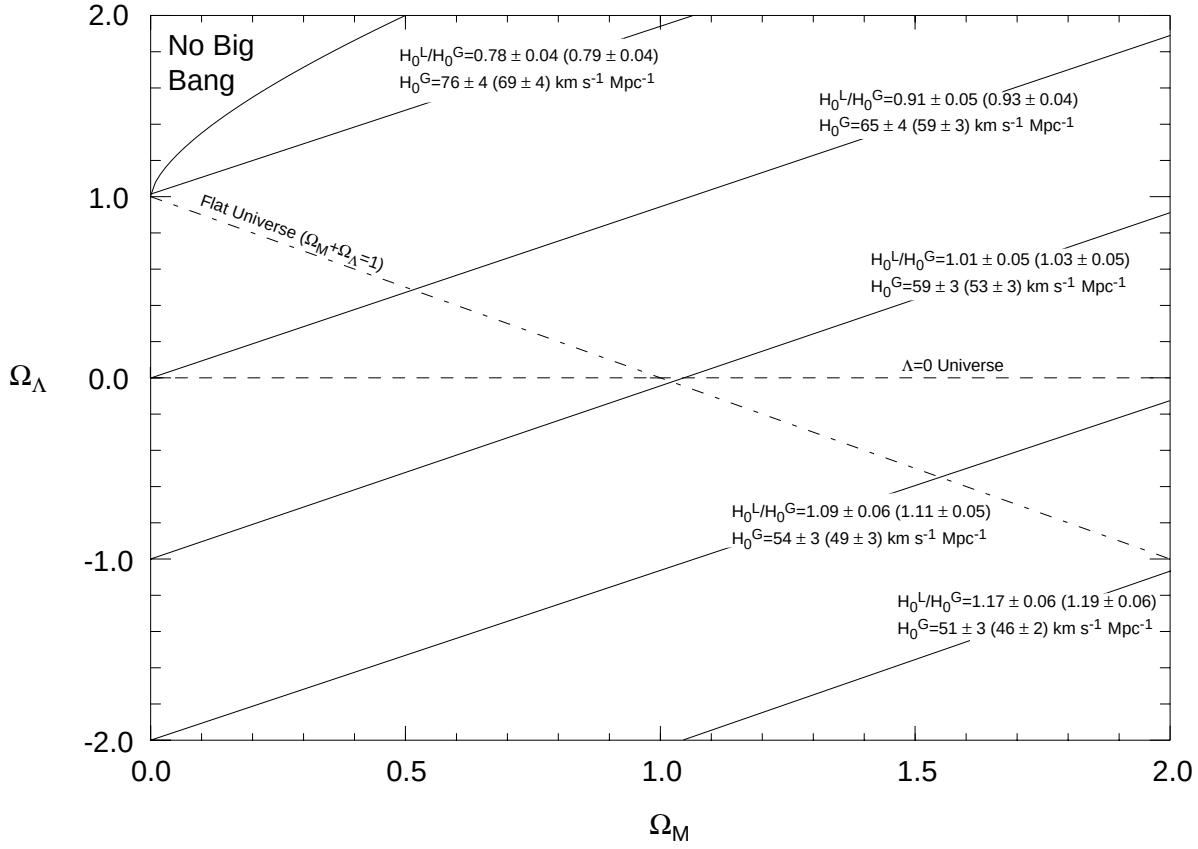


Fig. 3.— The solid lines show contours of constant $H_0^L/H_0^G$ and $H_0^G$ labeled with their appropriate errors in the $\Omega_M - \Omega_\Lambda$ plane for the five corrected SN magnitudes. The values of $H_0^L/H_0^G$ and $H_0^G$ derived from the seven non-corrected supernova magnitudes are given in parentheses for the approximately corresponding contour.